International Journal of Heat and Mass Transfer 52 (2009) 1734–1740

Contents lists available at ScienceDirect

International Journal of Heat and Mass Transfer

journal homepage: www.elsevier.com/locate/ijhmt

# Numerical analysis of an equivalent heat transfer coefficient in a porous model for simulating a biological tissue in a hyperthermia therapy

Ping Yuan *

*Mechanical Engineering, Lee Ming Institute of Technology, 2-2, Lee Zhuan Road, Taishan, Taipei 243, Taiwan, ROC*

ARTICLE INFO

*Article history:*
Received 30 April 2008
Received in revised form 25 September 2008
Available online 13 December 2008

*Keywords:*
Numerical analysis
Equivalent heat transfer coefficient
Porous model
Conjugate gradient method
Biological tissue
Hyperthermia

ABSTRACT

An equivalent heat transfer coefficient between tissue and blood in a porous model is investigated, which is applied to the thermal analysis of a biological tissue in a hyperthermia therapy. This paper applies a finite difference method to solving the tissue temperature distribution using Pennes' bio-heat transfer equation and a two-equation porous model, respectively, and then employs a conjugate gradient method to estimate the equivalent heat transfer coefficient in the two-equation porous model with a known perfusion rate in Pennes' bio-heat transfer equation. The results indicate that the equivalent heat transfer coefficient is not a strong function of the perfusion rate, blood velocity and heating conditions, but is inversely related to the blood vessel diameter.



## 1. Introduction

Hyperthermia therapy is a kind of method for enhancing the effect of radiotherapy and/or chemotherapy. Since Pennes [1] proposed a simple bio-heat equation model with a perfusion term, much of the literature on thermal model focuses on the validation of the perfusion term, and the simplicity of one governing equation. Weinbaum et al. [2] and Jiji et al. [3] proposed a new three-layer conceptual model supported by ultrastructure studies and high-spatial resolution temperature measurements. This model considered the variation in number density, size, and flow velocity of the countercurrent vessels as a function of depth from the skin, the directionality of blood perfusion in the transverse vessel layer and the superficial shunting of blood to the cutaneous layer. Wulff [4] used a local blood mass flux term instead of the perfusion rate term in bio-heat transfer to emphasize the directional blood flow effect. Weinbaum and Jiji [5] derived a new simplified three-dimensional bio-heat equation for describing the effect of blood flow on blood–tissue heat transfer. This model used the effective conductivity of the tissue as a function of local vascular geometry and flow velocity to describe an anisotropic heat transfer due to the incomplete countercurrent exchange in the thermally significant microvessels. Baish et al. [6] compared three different vascular models for describing heat transport in tissue, which are the bio-heat equation [1], the directed perfusion model [4], and the effective conductivity model [5]. Their study concluded that the directed perfusion or effective conductivity models would be applied to a tissue containing many small vessels, and suggested that the bio-heat equation is most appropriate for a tissue with a wide range of vessel sizes. Arkin et al. [7] reviewed many new bio-heat transfer models proposed by researchers from 1948 to 1994. Their comment was that the new models still lacked experimental grounding, and Pennes model might still be the best practical approach for modeling bio-heat transfer because of its simplicity. Consequently, most planning systems in hyperthermia treatment still utilize the bio-heat equation to calculate the temperature distribution because of the simplicity of this model [8–10].

Although Pennes model was recommended [7], and applied to many planning systems in hyperthermia therapy [8–10], its major drawback is that it cannot describe the effect of directional blood flow on temperature distribution because of the non-directional perfusion term in Pennes model. This means that the thermal contour is always symmetrical to the center point of the heating zone but does not move downstream, when a tissue has a directional blood flow. Therefore, many authors have investigated heat transfer in biological tissue using the theory of porous media. Khaled and Vafai [11] made a review on the role of porous media in modeling flow and heat transfer in biological tissues. They concluded that developing advanced heat transfer models according to the thermal non-equilibrium states between the blood and the tissue is an important task. Xuan and Roetzel [12] used the porous media concept to analyze the steady temperature distributions of tissue, artery and vein by a system of three energy equations. Although the governing equations are three-dimensional, they were simpli-

* Tel.: +886 2 29097811x2258; fax: +886 2 22966301.
*E-mail address:* pyuan@mail.lit.edu.tw

0017-9310/$ - see front matter © 2008 Elsevier Ltd. All rights reserved.
doi:10.1016/j.ijheatmasstransfer.2008.09.033

**Nomenclature**

| | |
|---|---|
| $a$ | volumetric heat transfer area ($m^2\ m^{-3}$) |
| $c_p$ | specific heat capacity ($J\ kg^{-1}\ ^\circ C^{-1}$) |
| $d_t$ | diameter of an equivalent circle tissue, as defined in Fig. 3 |
| $d_v$ | diameter of vessels, as shown in Fig. 3 |
| $h$ | heat transfer coefficient ($J\ m^{-2}\ s^{-1}$) |
| $k$ | conductivity ($J\ m^{-1}\ s^{-1}$) |
| $l_h$ | length of heating zone |
| $L$ | vessel distance |
| $q$ | absorbed power density ($W\ m^{-3}$) |
| $Q$ | blood flow rate ($m^3\ s^{-1}$) |
| $t$ | time (s) |
| $T$ | temperature (°C) |
| $u$ | blood velocity ($m\ s^{-1}$) |
| $w_b$ | perfusion rate ($kg\ s^{-1}$) |
| $x$ | $x$ direction |
| $y$ | $y$ direction |
| $z$ | $z$ direction |

*Greek symbols*

| | |
|---|---|
| $\rho$ | density ($kg\ m^{-3}$) |
| $\varepsilon$ | porosity |

*Subscript*

| | |
|---|---|
| b | blood |
| t | tissue |

fied into two-dimensional equations for tissue, and one-dimensional equations for bloods by analyzing an arm in the numerical method. Later, Roetzel and Xuan [13] extended their research to investigate the transient heat transfer problem between the artery, vein, and tissue with a cylinder physical model using the porous media concept. Meanwhile, the equations of arterial and venous blood are one-dimensional, which is the blood flow direction. The equation of tissue has two dimensions, which are the blood flow direction and radius. Kou et al. [14] have recently investigated the effect of directional blood flow on a three-dimensional thermal dose distribution during thermal therapy using Green's function method. This paper used the porous media concept and assumed local thermal equilibration to combine the energy conservation equations of tissue and blood into a single energy equation. The results showed that the domain of thermal lesion might extend to the downstream normal tissue if the porosity is high and the average blood velocity is of a larger value. Yuan [15] applied an evaluated heat transfer coefficient to a porous model for simulating a three-dimensional transient temperature distribution in a tissue with thermal non-equilibrium conditions. The thermal model considers the tissue with its blood vessel distribution as a porous medium and employs the convection term instead of the perfusion term in the energy conservation equations for both tissue and blood. In an accuracy comparison, the numerical results of this model were employed to compare with those obtained by the one-equation porous model under thermal equilibrium. The primary results indicate that the one-equation porous model will enhance the blood effect on temperature distribution when both blood vessel diameter and blood velocity increase.

Baish et al. used a parallel tube heat exchanger configuration to simulate the internal convection effects of blood flow [16]. The measured thermal response of a prototype compared favorably with the numerical solution of Pennes' bio-heat transfer equation (PBHTE). The results provided the relationships between tube size, spacing, and simulated perfusion rate. A porous model neglects the structure of blood vessel, and an energy conservation equation of blood with a porosity is then employed to treat the heat carried by blood. However, studies on the heat transfer coefficient between the tissue and blood in biological porous media in the literature are scarce. This induces an impropriety of applying the porous model to a biological tissue. Although this study had used a porous model to stimulate a transient temperature distribution in a tissue with thermal non-equilibrium conditions [15], the heat transfer coefficient cannot describe all kinds of heat exchange between a tissue and blood vessels of different diameters. In order to find a more reasonable heat transfer coefficient in porous media, this study considers a tissue with parallel straight vessels, whose size is identical to those in the reference of Baish et al. This study calculates the temperature distributions using Pennes' bio-heat transfer equation with the same conditions in the reference of Baish et al. and the porous equations with an assumed heat transfer coefficient. The conjugate gradient method is then employed to iterate previous calculations to pursue the final equivalent heat transfer coefficient between the tissue and blood in the porous media model. Because the temperature predicted by PBHTE had been verified by the experimental results of Baish et al., this equivalent heat transfer coefficient is valuable for applying the porous model to thermal analysis of a biological tissue.

## 2. Analysis

The transient temperature of a biological tissue in a hyperthermia therapy is investigated in this study. The whole calculation domain including tissue and blood is a cube with the length of 50 mm, and the heating zone is another cube with the length of 10 mm located in the center, as shown in Fig. 1. In this physical model, all blood vessels are straight in the $x$ direction, and the vessel diameter and vessel distance in Fig. 1 are listed in Table 1, which are the same design parameters as in [16]. In this study, the porous model assumes that blood vessels merge into the tissue, and this tissue becomes a bulk mixed with blood. Before formulating the governing equations, this study assumes that the thermal properties of tissue and blood are isotropic, and the heat transfer coefficient and blood velocity are constant throughout the entire calculation domain. Moreover, the metabolic heat generation is neglected because it is much smaller than the power density delivered from the ultrasound in hyperthermia treatment. Applying the conservation of energy to tissue and blood, this study builds a two-equation porous model (TEPM) as follows.

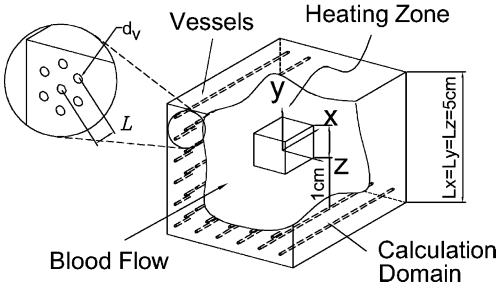


**Fig. 1.** Schematic diagram of a tissue with merged blood vessels in hyperthermal therapy ($d_v$: diameter of vessels, $L$: vessel distance).

**Table 1**
Comparison of parameters used in [16] and this study ($d_t$, diameter of an equivalent circle tissue; $d_v$, diameter of vessels; $w_b$, perfusion rate; $Q$, blood flow rate; $\varepsilon$, porosity; $u$, blood velocity; $a$, volumetric heat transfer area).

| Parameters in [16] | | | | Parameters in this study | | | |
|---|---|---|---|---|---|---|---|
| Case | $d_t$ (mm) | $d_v$ (mm) | $w_b$ (kg m$^{-3}$ s$^{-1}$) | $Q$ (mL s$^{-1}$) | $\varepsilon$ | $u$ (m s$^{-1}$) | $a$ (m$^2$ m$^{-3}$) |
| 1 | 19.82 | 2.28 | 1 | 15.59 | 0.013 | 3.80 | 23.27 |
| 2 | 14.42 | 2.28 | 2 | 8.25 | 0.025 | 2.01 | 43.97 |
| 3 | 12.06 | 2.28 | 3 | 5.77 | 0.036 | 1.41 | 62.86 |
| 4 | 10.48 | 2.28 | 4 | 4.36 | 0.048 | 1.06 | 83.13 |
| 5 | 9.92 | 2.28 | 5 | 3.90 | 0.053 | 0.95 | 93.09 |
| 6 | 17.83 | 1.14 | 1 | 12.61 | 0.0041 | 12.29 | 14.38 |
| 7 | 12.85 | 1.14 | 2 | 6.55 | 0.0079 | 6.38 | 27.70 |
| 8 | 10.75 | 1.14 | 3 | 4.59 | 0.0113 | 4.47 | 39.56 |
| 9 | 9.70 | 1.14 | 4 | 3.73 | 0.0139 | 3.64 | 48.58 |
| 10 | 8.65 | 1.14 | 5 | 2.97 | 0.0175 | 2.90 | 61.07 |
| 11 | 20.98 | 4.56 | 1 | 17.46 | 0.0475 | 1.06 | 41.57 |
| 12 | 15.73 | 4.56 | 2 | 9.82 | 0.0845 | 0.60 | 73.90 |
| 13 | 13.58 | 4.56 | 3 | 7.32 | 0.1133 | 0.45 | 99.14 |
| 14 | 12.06 | 4.56 | 4 | 5.77 | 0.1437 | 0.35 | 125.72 |
| 15 | 11.27 | 4.56 | 5 | 5.04 | 0.1645 | 0.31 | 143.88 |

$$(1-\varepsilon)(\rho c_p)_t\frac{\partial T_t}{\partial t}=(1-\varepsilon)k_t\left(\frac{\partial^2 T_t}{\partial x^2}+\frac{\partial^2 T_t}{\partial y^2}+\frac{\partial^2 T_t}{\partial z^2}\right)+ha(T_b-T_t)+(1-\varepsilon)q_t \quad (1)$$

$$\varepsilon(\rho c_p)_b\frac{\partial T_b}{\partial t}+\varepsilon(\rho c_p)_b\left(u\cdot\frac{\partial T_b}{\partial x}\right)=\varepsilon k_b\left(\frac{\partial^2 T_b}{\partial x^2}+\frac{\partial^2 T_b}{\partial y^2}+\frac{\partial^2 T_b}{\partial z^2}\right)+ha(T_t-T_b)+\varepsilon q_b \quad (2)$$

Here, $\varepsilon$ is the porosity, which is the ratio of blood volume to total volume, $\rho$ is the density, $c_p$ is the specific heat capacity, $k$ is the thermal conductivity, $h$ is the heat transfer coefficient, $u$ is the blood velocity, $a$ is the volumetric transfer area between tissue and blood, and $q$ is the absorbed power density. Moreover, subscripts $t$ and $b$ represent tissue and blood, respectively. In Fig. 1, the inlet temperature of blood and the boundary temperature of the calculation domain are 37 °C.

Moreover, this study also uses Pennes' bio-heat transfer equation (PBHTE) to predict the temperature distribution of the physical model in Fig. 1.

$$(\rho c_p)\frac{\partial T_t}{\partial t}=k\left(\frac{\partial^2 T_t}{\partial x^2}+\frac{\partial^2 T_t}{\partial y^2}+\frac{\partial^2 T_t}{\partial z^2}\right)+w_b\cdot c_p(T_a-T_t)+q \quad (3)$$

The above Eq. (3) is the well-known Pennes' bio-heat transfer equation. Meanwhile, $w_b$ is the perfusion rate, $T_a$ is the artery temperature, and $q$ is the absorbed power density of tissue. In this study, $T_a$ is set to be 37 °C.

## 3. Numerical methods

This study discretizes Eqs. (1)–(3) into finite difference equations with an implicit scheme, and then employs the Tri-Diagonal Matrix Algorithm (TDMA) to solve the tissue and blood temperature from the finite difference equations of Eqs. (1) and (2), as well as the tissue temperature from the finite difference equation of Eq. (3), respectively. The grid dimension is selected to be 60 × 60 × 60 for calculating the temperature response of the tissue. On the other hand, this study also uses FlexPDE software to solve the governing equations, because the package is a flexible solver for partial differential equations. Fig. 2 compares the results calculated by this numerical program with those calculated by FlexPDE software for the two-equation porous model (TEPM) under different blood velocities and porosities when the heating duration is 10 s and the heating power density is $3\times10^6$ W m$^{-3}$. In this figure, the lines and closed circles stand for the results of the numerical method in this study and obtained by FlexPDE software, respectively, and both of them match with each other in each case. Therefore, this establishes the reliability of the numerical method of this study for solving 3D temperature distribution.

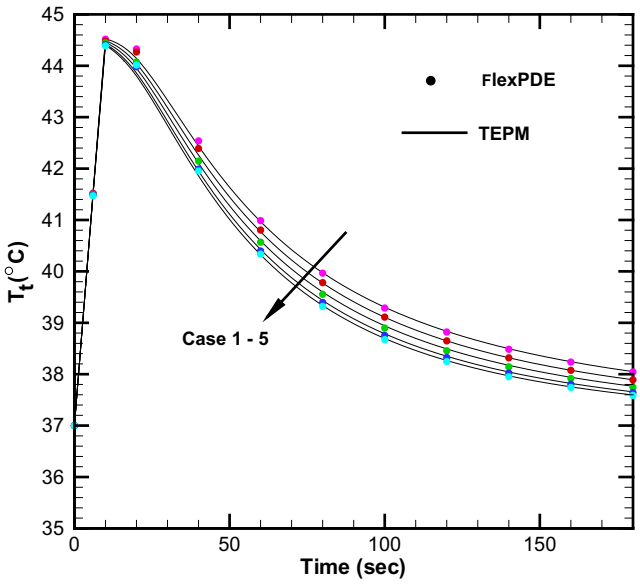


**Fig. 2.** Comparison of accuracy in calculating central tissue temperature obtained in this study and using numerical package for two-equation porous model for different cases when the heating duration is 10 s and heating power density is $3\times10^6$ W m$^{-3}$.

The conjugate gradient method is an inverse method for finding the minimum of an objective function. In this study, the Fortran program first calculates the tissue temperature in Pennes' bio-heat transfer equation and the two-equation porous model with a guessed heat transfer coefficient, respectively. Then, the program calculates an objective function defined as follows.

$$J=\sum_{t=1}^{180}\left(T_{t,TEPM}(0,0,0,t,h^n)-T_{t,PBHTE}(0,0,0,t,w_b)\right)^2 \quad (4)$$

The superscript $n$ represents the $n$th iteration. This study gives a perturbation of heat transfer coefficient to solve a new tissue temperature in Eqs. (1) and (2), which can then obtain the temperature gradient in the two-equation porous model as follows.

$$\frac{\partial T_{t,TEPM}}{\partial h}=\frac{T_{t,TEPM}(h^n+\Delta h)-T_{TEPM}(h^n)}{\Delta h} \quad (5)$$

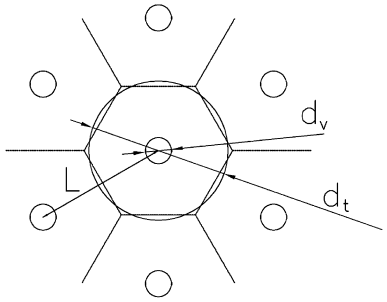


**Fig. 3.** Repeated hexagon unit with the structure of a tissue and a blood vessel in the $y$–$z$ plane.

The conjugate gradient method for minimization is

$$h^{n+1} = h^n - \beta^n p^n \tag{6}$$

Here, $\beta^n$ is the step size of the $n$th iteration, and $p^n$ is the descent direction of the $n$th iteration defined as follows.

$$p^n = \left(\frac{\partial J}{\partial h}\right)^n + \gamma^n p^{n-1} \tag{7}$$

The coefficient of conjugate gradient, $\gamma$, is defined as follows.

$$\gamma^n = \frac{\left[\left(\frac{\partial J}{\partial h}\right)^n\right]^2}{\left[\left(\frac{\partial J}{\partial h}\right)^{n-1}\right]^2} \tag{8}$$

Then, the step size can be derived by minimizing the objective function as follows.

$$\beta^n = \frac{\sum_{t=1}^{180}\left[T_{t,TEPM}(h^n) - T_{t,PBHTE}\left(\frac{\partial T}{\partial h}\right)^n p^n\right]\Delta t}{\sum_{t=1}^{180}\left[\left(\frac{\partial T}{\partial h}\right)^n p^n\right]^2 \Delta t} \tag{9}$$

This study iterates the calculations from Eqs. (4)–(9) till the following criterion is satisfied, and then gets the equivalent heat transfer coefficient.

$$J(h^{n+1}) < \delta \tag{10}$$

where $\delta$ is a small positive value.

## 4. Results and discussion

Thermal conductivity values of tissue and blood of 0.5 W m$^{-1}$ °C$^{-1}$, the density of tissue and blood of 1050 kg m$^{-3}$, and the specific heat capacity of tissue and blood of 3770 J kg$^{-1}$ °C$^{-1}$ were selected. Three heating conditions were considered: 2-s heating with a power density of $1.5 \times 10^7$ W m$^{-3}$, 10-s heating with a power density of $3 \times 10^6$ W m$^{-3}$, and 50-s heating with a power density of $6 \times 10^5$ W m$^{-3}$. All of these heating conditions have the same input energy of $3 \times 10^7$ J m$^{-3}$, which can raise the tissue temperature to 45 °C with adiabatic boundary conditions. Because vessels are uniformly distributed in the tissue, the whole domain can be considered as an assembly of repeated hexagon units, as shown in Fig. 3. Meanwhile, $d_t$ is the diameter of an equivalent circle tissue, $d_v$ is the diameter of vessels, and $L$ is the vessel distance. The relationship between $d_t$ and $L$ is as follows.

$$d_t = 1.05L \tag{11}$$

Table 1 lists parameters cited from [16] in the left columns and the derived parameter applied to the porous model in the right columns. In Table 1, $w_b$ is the perfusion rate from the experiment result [16], and $Q$ is the blood flow rate. The blood flow rate must be high enough to prevent a significant rise in temperature along the length of the vessel for satisfying the constant artery temperature in the perfusion term of PBHTE. This flow rate under a steady con-

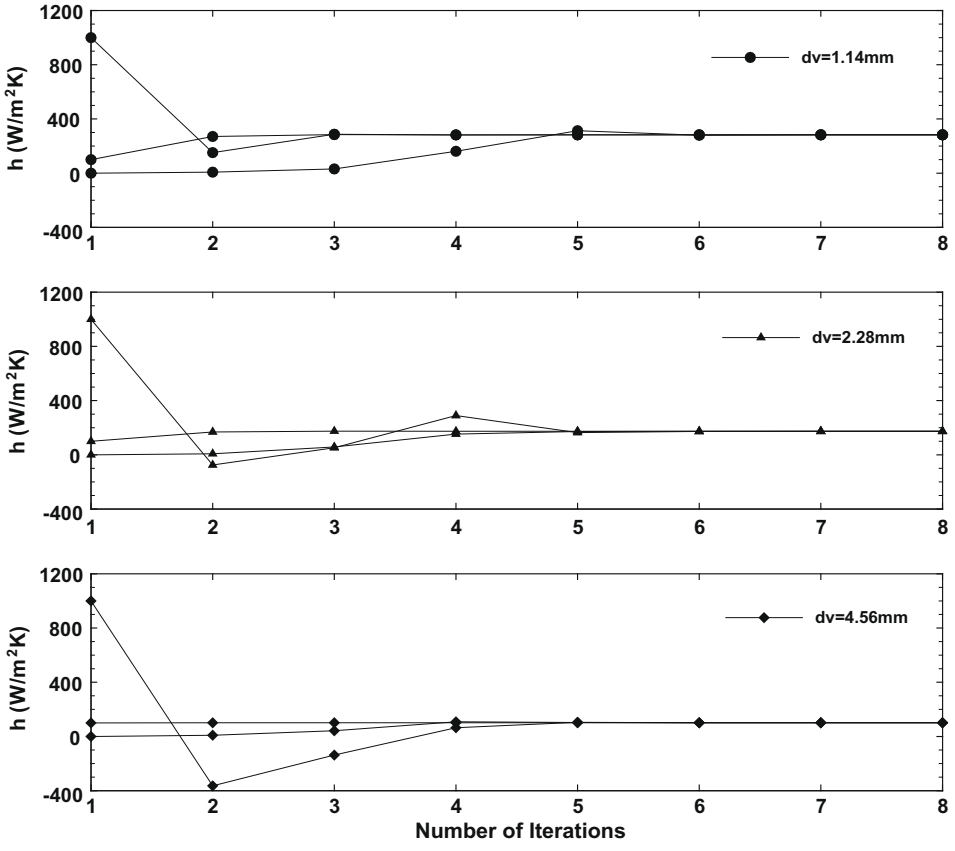


**Fig. 4.** Effect of initial guessed value on the convergence speed for blood vessels of different diameters.

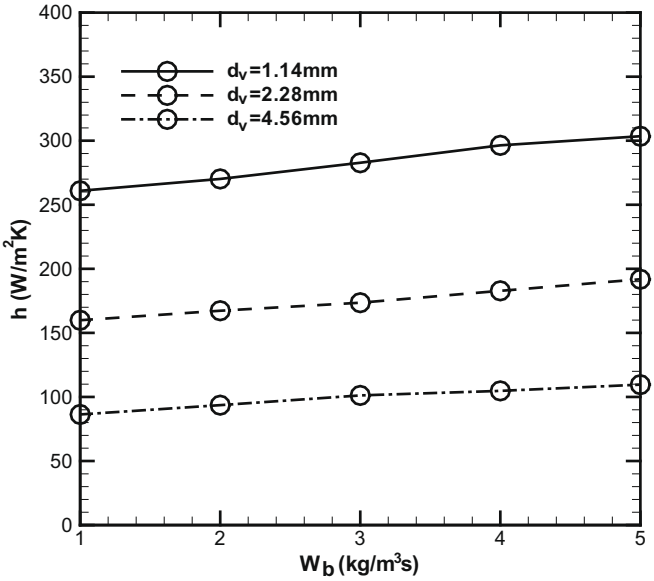


**Fig. 5.** Equivalent heat transfer coefficient in TEPM related to the perfusion rate in PBHTE through calculation of the inverse method.

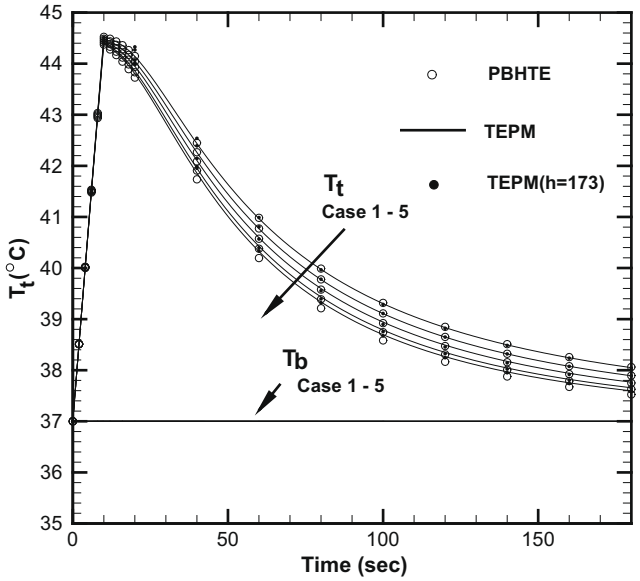


**Fig. 6.** Tissue and blood temperature responses in the central point with equivalent heat transfer coefficients when the blood diameter is 2.28 mm.

dition is in terms of a given rise in temperature, heated volume, and heat generation rate.

$$Q = \frac{\pi \cdot l_h \cdot d_t^2 \cdot q}{4\rho_b c_b \cdot \Delta T} = \frac{\pi d_t^2 u}{4} \tag{12}$$

where $l_h$ is the length of heating zone, and $\Delta T$ is the rise in blood temperature. Here, $l_h$ is 1 cm, $\Delta T$ is 0.5 °C, and $q$ is $10^7$ W m$^{-3}$. Additionally, the derived parameters in the right columns of Table 1, $\varepsilon$, $u$, and $a$, can be calculated from the values of parameter $d_t$, $d_v$, and $Q$.

Fig. 4 depicts the number of convergent iterations with different initial guesses of an equivalent heat transfer coefficient in Cases 3, 8, and 13 of Table 1. It is clear that the number of convergent iterations is only 2 when the guessed value is 100, whereas the number of convergent iterations will increase to 5 when the guessed value is 0 and 1000. Therefore, this study sets the guessed value to be 100 in the inverse method for calculating all cases in Table 1. Moreover, this figure implies that the local minimization of objective function is valid between $h = 0$ and $h = 1000$ in this inverse method. Fig. 5 shows the equivalent heat transfer coefficient versus the perfusion rate at different blood vessel diameters. Meanwhile, the solid, dashed, and dash-dotted line represent the results when $d_v = 1.14$, 2.28, and 4.56 mm, respectively. In this figure, the equivalent heat transfer coefficient increases obviously with a decrease in vessel diameter, and is slightly affected by the change in perfusion rate. When the diameter of blood vessel is 1.14, 2.28, and 4.56 mm, the average equivalent heat transfer coefficient is close to 99, 173, and 285 W m$^{-2}$ °C$^{-1}$, respectively.

Fig. 6 depicts the response of tissue and blood temperature to time for different cases when $d_v$ is 2.28 mm. As can be seen, the variation in blood temperature is below 0.5 °C and satisfies the hypothesis for estimating the blood velocity in Eq. (12). This means that the flow rate is high enough to prevent a significant rise in blood temperature along the length of the vessel. Moreover, this figure examines the central tissue temperature response calculated by TEPM and PBHTE, respectively. This study calculates the tissue temperature in TEPM using the equivalent heat transfer coefficient, and that in PBHTE using the blood perfusion rate. In this figure, it is clear that all open circles match the continuous line well. Moreover, the closed circles stand for the central tissue temperature response for Cases 1–5 calculated by TEPM using the average heat transfer coefficient of 173 W m$^{-2}$ °C$^{-1}$, and these closed circles are close to the continuous line. This means that the average heat transfer coefficient obtained in Fig. 5, $h = 99$, 173, and 285, can be set in the calculations of Cases 6–10, Cases 1–5, and Cases 11–15, respectively. Note that the inverse method uses only the central tissue temperature as the objective function, and it cannot prove that the temperature distribution calculated by TEPM is identical to that calculated by PBHTE even when the equivalent heat transfer coefficient related to the perfusion rate has been evaluated. Therefore, this study depicts the tissue temperature distributions of Case 3 at $t = 25$ s calculated by both TEPM and PBHTE in Fig. 7. The result indicates that the tissue temperature distribution predicted by TEPM using the equivalent heat transfer coefficient is identical to that predicted by PBHTE using the blood perfusion rate.

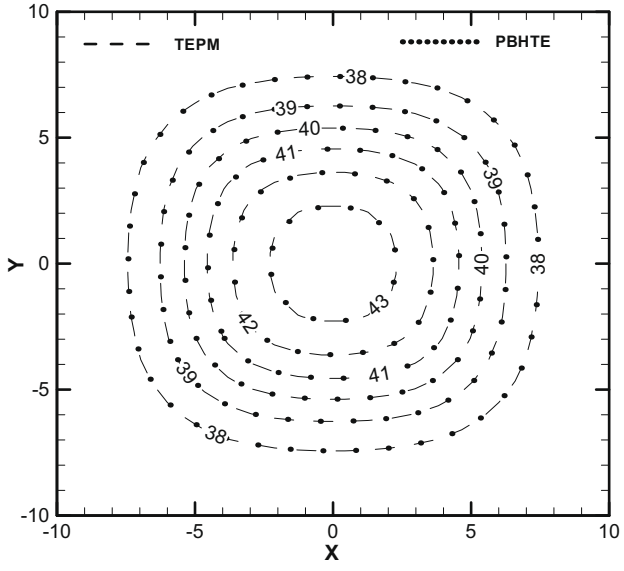


**Fig. 7.** Comparison of tissue temperature distribution calculated by PBHTE and TEPM at $t = 25$ s.

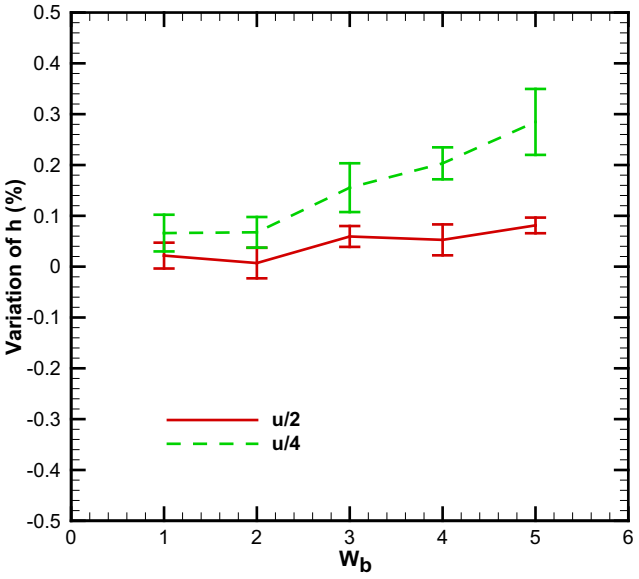


**Fig. 8.** Variation in equivalent heat transfer coefficient with respect to change in blood velocity when blood vessel diameter is between 1.14 and 4.56 mm.

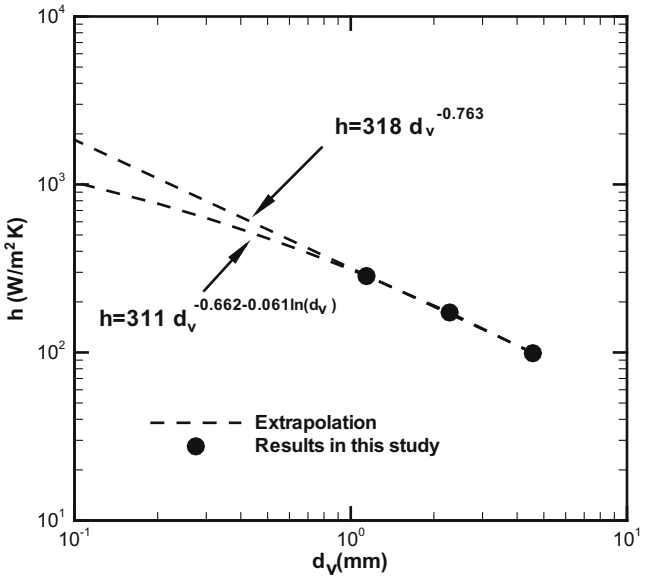


**Fig. 10.** Relationships between equivalent heat transfer coefficient and blood vessel diameter.

Consequently, the equivalent heat transfer coefficient obtained by the inverse method using the central tissue temperature as the objective function is suitable for calculating in TEPM for the whole domain.

Fig. 8 depicts the variation in equivalent heat transfer coefficient with respect to change in blood velocity for blood vessels of different diameters. Each vertical bar represents range of heat transfer coefficient when the blood diameter is between 1.14 and 4.56 mm. The continuous line and dashed line stand, respectively, for the results when the blood velocity is half and quarter of the original velocity calculated from Eq. (12), as listed in Cases 1–5 of Table 1. In this figure, all variations are less than 0.5%, so the equivalent heat transfer coefficient is not a strong function of blood velocity. Fig. 9 shows the variation in equivalent heat transfer coefficient with respect to different heating conditions when the blood vessel diameter is 1.14, 2.28, and 4.56 mm. The continuous line and dashed line represent the results when the heating time is 50 s and the power density is $6 \times 10^5$ W m$^{-3}$, as well as the heating time is 2 s and power density is $1.5 \times 10^7$ W m$^{-3}$, respectively. As can be seen, the equivalent heat transfer coefficient is not a strong function of the heating conditions because all the variations are less than 0.5%. According to the results in Figs. 5, 8, and 9, this study can conclude that the equivalent heat transfer coefficient is dominantly affected by the change in blood vessel diameter, and slightly affected by the changes in perfusion rate, blood velocity, and heat conditions. Consequently, this study tries to obtain the relationship between the equivalent heat transfer coefficient and the blood vessel diameter.

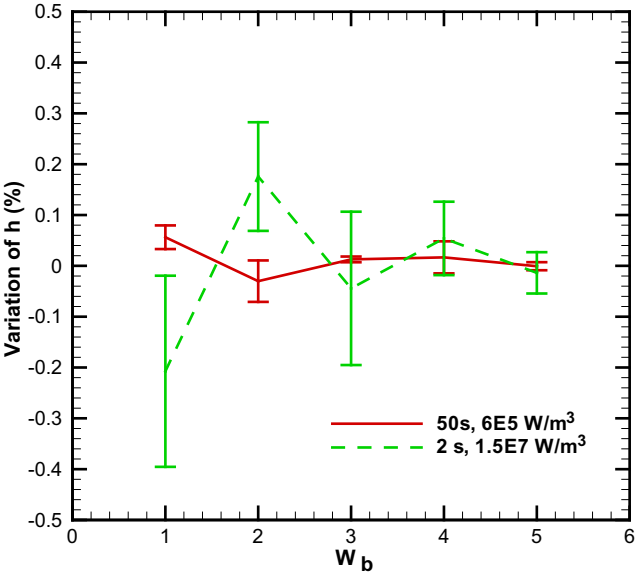


**Fig. 9.** Variation in equivalent heat transfer coefficient with respect to change in heating condition when blood vessel diameter is between 1.14 and 4.56 mm.

Fig. 10 plots the average equivalent heat transfer coefficients with closed circles at $d_v$ = 1.14, 2.28, and 4.56 mm, which are obtained from Fig. 5. As can be seen, there exists a linear relationship between the blood vessel diameter and the equivalent heat transfer coefficient in the axis with logarithm scale. This study uses the curve fitting skill to obtain the relationship in terms of a first-order and a second-order polynomial curve, and draws the curve to extend smaller blood vessels. The curve fitting formula in the first-order and the second-order polynomial are as follows.

$$h = 318 d_v^{-0.763} \tag{13}$$

$$h = 311 d_v^{-0.662-0.061\ln(d_v)} \tag{14}$$

The relative errors of Eqs. (13) and (14) are found to be 2% and 0.001%, respectively. Eq. (13) is built according to a hypothesis of linear relationship between the logarithm of $h$ and $d_v$, and it is simpler for application, whereas Eq. (14) maybe more accurate when we extend the vessel diameter range of 1.14–4.56 mm in the experiment of Baish et al. [16] to the range of 0.1–1 mm, because it has smaller relative error when $d_v$ is larger than 1 mm. Note that it is necessary to verify the equivalent heat transfer coefficient at a vessel diameter less than 1 mm by experiments, before the TEPM applying on the thermal analysis of a tissue with smaller vessel distribution in hyperthermia therapy.

## 5. Summary

Most planning systems in hyperthermia treatment still utilize the Pennes bio-heat transfer equation (PBHTE) to calculate the temperature distribution because of the simplicity of this model. However, its major drawback is that it cannot describe the effect of directional blood flow on temperature distribution because of the non-directional perfusion term in its model. The two-equation porous model (TEPM) can describe the effect of directional blood on the temperature distribution, but it needs a reasonable heat transfer coefficient in porous media, which is scarce in the literature. Therefore, this study investigated an equivalent heat transfer coefficient between a biological tissue and blood when the blood vessels merge into the tissue and appear to be a porous medium. According to the experimental structure in the literature, this study can calculate the relative values of porosity, volumetric transfer area, and blood velocity in the porous model. Through an application of the conjugate gradient method, this paper found that the equivalent heat transfer coefficient in the porous model corresponds to the blood perfusion rate in Pennes' bio-heat transfer equation applied to the experimental structure in previous studies. The results indicate that the heat transfer coefficient between the tissue and blood in the porous model is between 100 and 300 $W\,m^{-2}\,°C^{-1}$ when the perfusion rate is in a range of 1–5 $kg\,m^{-3}\,s^{-1}$ and the vessel diameter is larger than 1.14 mm. This equivalent heat transfer coefficient is slightly affected by the perfusion rate, and is independent of blood velocity and heating conditions, yet increases apparently with a decrease in blood vessel diameter. This study applied a curve fitting scheme to find a first-order and a second-order polynomial curve, respectively, to describe the relationship between the equivalent heat transfer coefficient and vessel diameter in the porous media model, which curve formulas have a relative error below 2%. Therefore, the TEPM can be applied to the thermal analysis of a tissue in the hyperthermia therapy through the accurate equivalent heat transfer coefficient calculated using the equivalent heat transfer coefficient formula. It is noted that the equivalent heat transfer coefficients at vessel diameter more than 1 mm are derived from the experiment results of the literature [16], and the future research will focus on experimental validation of the equivalent heat transfer coefficient formula when the vessel diameter is in the range of micro vascular.

## Acknowledgement

The authors thank the National Science Council of the Republic of China, Taiwan, for the financial support of this research under Contract No. NSC94-2213-E-234-003.

## References

[1] H.H. Pennes, Analysis of tissue and arterial blood temperatures in the resting human forearm, J. Appl. Physiol. 1 (1948) 93–122.
[2] S. Weinbaum, L.M. Jiji, D.E. Lemons, Theory and experiment for the effect of vascular microstructure on surface tissue heat transfer. Part I: Anatomical foundation and model conceptualization, J. Biomech. Eng.: Trans. ASME 106 (1984) 321–330.
[3] L.M. Jiji, S. Weinbaum, D.E. Lemons, Theory and experiment for the effect of vascular microstructure on surface tissue heat transfer. Part II: Model formulation and solution, J. Biomech. Eng.: Trans. ASME 106 (1984) 331–341.
[4] W. Wulff, The energy conservation equation for living tissue, IEEE Trans. Biomed. Eng. 21 (1974) 494–495.
[5] S. Weinbaum, L.M. Jiji, A new simplified bioheat equation for the effect of blood flow on local average tissue temperature, J. Biomech. Eng.: Trans. ASME 107 (1985) 131–139.
[6] J.W. Baish, P.S. Ayyaswamy, K.R. Foster, Heat transport mechanisms in vascular tissues: a model comparison, J. Biomech. Eng.: Trans. ASME 108 (1986) 324–331.
[7] H. Arkin, L.X. Xu, K.R. Holmes, Recent developments in modeling heat transfer in blood perfused tissues, IEEE Trans. Biomed. Eng. 41 (1994) 97–107.
[8] G. Sreenivasa, J. Gellermann, B. Rau, J. Nadobny, P. Schlag, P. Deuflhard, R. Felix, P. Wust, Clinical use of the hyperthermia treatment planning system hyperplan to predict effectiveness and toxicity, Int. J. Radiat. Oncol. Biol. Phys. 55 (2003) 407–419.
[9] P. Marinia, C. Guiota, B. Baiotto, P. Gabriele, PC-aided assessment of the thermal performances of a MW applicator for oncological hyperthermia, Comput. Biol. Med. 34 (2004) 3–13.
[10] F.S. Gayzik, E.P. Scott, T. Loulou, Experimental validation of an inverse heat transfer algorithm for optimizing hyperthermia treatments, J. Biomech. Eng.: Trans. ASME 128 (2006) 505–515.
[11] A.R.A. Khaled, K. Vafai, The role of porous media in modeling flow and heat transfer in biological tissues, Int. J. Heat Mass Transfer 46 (2003) 4989–5003.
[12] Y. Xuan, W. Roetzel, Bioheat equation of the human thermal system, Chem. Eng. Technol. 20 (1997) 268–276.
[13] W. Roetzel, Y. Xuan, Transient response of the human limb to an external stimulant, Int. J. Heat Mass Transfer 41 (1998) 229–239.
[14] H.S. Kou, T.C. Shih, W.L. Lin, Effect of the directional blood flow on thermal dose distribution during thermal therapy: an application of a Green's function based on the porous model, Phys. Med. Biol. 48 (2003) 1577–1589.
[15] P. Yuan, Numerical analysis of temperature and thermal dose response of biological tissues to thermal non-equilibrium during hyperthermia therapy, Med. Eng. Phys. 30 (2008) 135–143.
[16] J.W. Baish, K.R. Foster, P.S. Ayyaswamy, Perfused phantom models of microwave irradiated tissues, J. Biomech. Eng.: Trans. ASME 108 (1986) 239–245.